A Novel Blood Glucose Regulation Using TSK^0-FCMAC: A Fuzzy CMAC Based on the Zero-Ordered TSK Fuzzy Inference Scheme

Chan Wai Ting and Chai Quek, *Member, IEEE*

***Abstract*—This paper presents a novel blood glucose regulation for type I (insulin-dependent) diabetes mellitus patients using biologically inspired TSK^0-FCMAC, a fuzzy cerebellar model articulation controller (CMAC) based on the zero-ordered Takagi–Sugeno–Kang (TSK) fuzzy inference scheme. TSK^0-FCMAC is capable of performing localized online training with an effective fuzzy inference scheme that could respond swiftly to changing environment such as human's endocrine system. Without prior knowledge of disturbance (e.g., food intake), the proposed fuzzy CMAC is able to capture the glucose-insulin dynamics of individuals under different dietary profiles. Preliminary simulations show that the blood glucose level is kept within the state of euglycemia. The design of the proposed system follows closely to what is available in real life and is suitable for animal and clinical pilot testing in the near future.**

***Index Terms*—Blood glucose regulation, diabetes type I, dietary profile, intra- and interpatient metabolic variation, localized memory structure, model reference neural adaptive control, Takagi–Sugeno–Kang (TSK) fuzzy inference scheme, TSK^0-FCMAC.**

I. Introduction

TYPE I or insulin-dependent diabetes mellitus is a chronic disease that occurs when the pancreas does not produce sufficient insulin. Prolonged period of hyperglycemia, or raised blood sugar, is a common effect of uncontrolled diabetes, which may lead to serious damage to many of the body's systems, especially the nerves, eye, and kidney. On the other hand, hypoglycemia, or low blood sugar, may cause unconsciousness, brain damage, or even death in some severe cases. The World Health Organization (WHO) estimates that more than 180 million people worldwide have diabetes and this number is likely to more than double by 2030. In 2005, an estimated 1.1 million people died from diabetes [1].

As diabetic cases are expected to increase in future, blood glucose regulation has been an active research field over the years. Despite various attempts by researchers, the constraints of having limited information on current blood glucose level restricted superior results in this field. With the emergence of new electroenzymatic manufacturing technique [2], [3], the glucose concentration can now be estimated through measuring the catalyzed production of hydrogen peroxide. As a result, a spinoff commercial product MiniMed [4] enables subcutaneous glucose measurement at 5-min intervals. This advancement in sensor technology dramatically changes the research effort and direction in glucose–insulin dynamics. A significant amount of research has been carried out since then with this newly available information in blood glucose regulation.

Early research efforts focused on mathematical modeling of glucose–insulin dynamics [5]–[9]. Based on these mathematical models, some educational simulators are developed [10], [11]. Many other researchers tried to handle blood glucose regulation with expert systems [12], model-based predictive control algorithm [13], [14], proportional–integral–derivative (PID) control systems [15], H^∞ optimal control [16], [17], parametric programming [18], neural networks [19]–[22], or fuzzy-based controller [23]. However, the following important constraints are neglected.

- Disturbance (e.g., food intake): Most previous works assume the diabetic patient to have regular food intake at fixed timing. Some of these works may even employ the amount of food intake, meal time, or time of the day as part of the input to their system. However, the accuracy of information such as food intake is highly dependent on the self-discipline of a patient. They are also susceptible to human mistakes, especially for adolescent patients.
- Personalized glucose–insulin dynamics: Instead of adapting to glucose–insulin dynamics of individual, set of parameters is identified by defining various assumptions. Thus, the response of the system is bounded at the expense of optimal result. These systems do not perform online training and hence are nonadaptive to vibrant environment such as human's endocrine system.

In this paper, we propose a novel blood glucose regulation using TSK^0-FCMAC, a brain inspired cerebellar-like fuzzy association memory based on the zero-ordered Takagi–Sugeno–Kang fuzzy inference scheme [24], [25]. The proposed system is able to perform online learning without the need of prior knowledge of food intake. Preliminary simulations show that the proposed system is able to adapt to both intra- and interpatient variations.

Manuscript received February 16, 2008; revised November 19, 2008; accepted December 02, 2008. First published March 16, 2009; current version published May 01, 2009.

The authors are with the Centre of Computational Intelligence, School of Computer Engineering, Nanyang Technological University, Singapore 639798, Singapore (e-mail: tingchanwai@pmail.ntu.edu.sg; ashcquek@ntu.edu.sg).

Color versions of one or more of the figures in this paper are available online at http://ieeexplore.ieee.org.

Digital Object Identifier 10.1109/TNN.2008.2011735

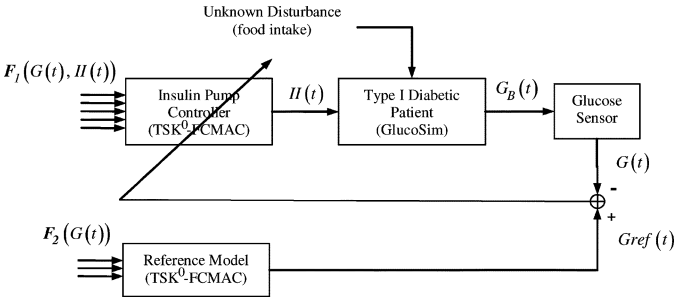

Fig. 1. Block diagram for closed-loop blood glucose control system. $G_B(t)$ represents the actual plasma glucose level; $G(t)$ represents the output from the glucose sensor; $G\mathrm{ref}(t)$ represents the output from the reference model; $II(t)$ represents the insulin infusion rate of the insulin pump; $\mathtt{F}_1(G(t), II(t))$ represents the inputs of the controller and they are derived from historical values of $G(t)$ and $II(t)$; $\mathtt{F}_2(G(t))$ represents the inputs of the reference model and they are derived from historical readings of $G(t)$.

II. System Description

A closed-loop blood glucose control system consists of four components, namely: 1) patient model, 2) glucose sensor, 3) insulin infusion pump with controller, and 4) reference model. The block diagram for the proposed system is shown in Fig. 1. In the proposed system, the patient model is simulated by a web-based educational simulation package GlucoSim [10], [26]. The glucose sensor is an enzymatic electrochemical sensor that is inserted into the subcutaneous area. The blood glucose level is estimated through measurement of the electric current generated when chemical reaction is catalyzed by an enzyme called glucose oxidase [4]. The reference model provides reference blood glucose level for the controller of the insulin pump. Both the reference model and the controller are modeled by a TSK^0-FCMAC network.

A. GlucoSim

GlucoSim, a web-based educational simulation package for glucose–insulin levels in the human body from Illinois Institute of Technology (Chicago, IL), is employed in this study [10], [26]. Based on the mathematical models by Sorensen [7] and Puckett [9], the simulator can provide virtual experiments to simulate blood glucose and insulin dynamics in healthy individuals and type I diabetes patients under different dietary profile.

The main disadvantage of the simulated model is that the personal variations in physiological parameters are not taken into account. Therefore, the outputs are merely average values [26]. Thus, body weight is the only parameter that can be adjusted to simulate individuals of different profiles with GlucoSim. In our experiments, GlucoSim is used to simulate a detailed model based on Puckett's work [9].

B. TSK^0-FCMAC

The conventional CMAC network is a uniformly quantized lookup table with black box operation. The memory efficiency is limited by its rigid structure. In this paper, a new class of brain inspired CMAC, referred to as TSK^0-FCMAC is proposed. Fuzzy inference model has been successfully incorporated into the CMAC networks whereby fuzzy rules could be generated to interpret the operation of the network. TSK^0-FCMAC employs discrete incremental clustering (DIC) technique [27] that enables the CMAC network to grow without prior knowledge of the number of clusters. The antecedent and consequent of the fuzzy model are represented by membership function that is highly computational efficient. In addition, the learning convergence of TSK^0-FCMAC has been established in [28] and [29]. The ability of TSK^0-FCMAC to perform localized online training, coupled with swift response against changing environment, fulfills the necessary requirements in blood glucose regulation. The network structure and the learning algorithm of the proposed architecture are presented in the following section.

1) Network Structure: Most neural fuzzy inference systems use complex function to represent the antecedent, such as bell-shaped membership function (Ker's FCMAC [30]) and Gaussian membership function (Kim's HyFIS [31] and Jang's ANFIS [32]), to generate smoother approximation. Instead of adopting these complex functions, the antecedents for TSK^0-FCMAC are represented in triangular or trapezoidal membership functions. Thus, accuracy is sacrificed for simplicity and computational efficiency. The consequent can be represented by crisp, fuzzy, and functional consequents. Each type of rule consequent has its merits. Neural fuzzy inference systems such as GenSoFNN [33], Falcon-ART [34], and Falcon-MART [35] adopt fuzzy consequent for higher suitability to capture imprecise human expertise. ANFIS, another prominent neural fuzzy inference system, employs functional consequent for accuracy using a small number of rules. Instead of a functional consequent, TSK^0-FCMAC employs crisp consequent (also called *fuzzy singleton*) for efficiency in computation. As a result, TSK^0-FCMAC is equivalent to zero-ordered TSK inference model.

For simplicity, the structure under consideration in this section has two inputs x_1 and x_2 and one output y. Consider the presentation of the sth sample in the tth iteration and assume the fuzzy inference rule base contains two fuzzy IF–THEN rules of TSK's type [24], [25], R_1 and R_2 defined in

$$R_1: \text{IF } x_1 \text{ is } A_{1,j}^{(1)} \text{ and } x_2 \text{ is } A_{2,j}^{(1)}, \quad \text{THEN } y_s^{(1)}(t) = b_{0,s}^{(1)}(t) + b_{1,s}^{(1)}(t)x_1 + b_{2,s}^{(1)}(t)x_2 \quad (1)$$

$$R_2: \text{IF } x_1 \text{ is } A_{1,j}^{(2)} \text{ and } x_2 \text{ is } A_{2,j}^{(2)}, \quad \text{THEN } y_s^{(2)}(t) = b_{0,s}^{(2)}(t) + b_{1,s}^{(2)}(t)x_1 + b_{2,s}^{(2)}(t)x_2 \quad (2)$$

where $A_{i,j}^{(k)}$ is the jth fuzzy set of the ith input that is connected to R_k; $y_s^{(k)}(t)$ is the output of kth fuzzy IF–THEN rule at the presentation of the sth sample in the tth iteration; $b_{j,s}^{(k)}(t)$ is the jth data content of the kth fuzzy IF–THEN rule at the presentation of the sth sample in the tth iteration; $A_{1,j}^{(1)}$, $A_{2,j}^{(1)}$, $A_{1,j}^{(2)}$, and $A_{2,j}^{(2)}$ are fuzzy sets; and $b_{0,s}^{(1)}(t)$, $b_{1,s}^{(1)}(t)$, $b_{2,s}^{(1)}(t)$, $b_{0,s}^{(2)}(t)$, $b_{1,s}^{(2)}(t)$, and $b_{2,s}^{(2)}(t)$ are real-valued parameter. The total output of the model $y_s(t)$ is described by (3), shown at the bottom of the next page, where N_R is the total number of rules, and $\alpha_s^{(k)}$ is the degree of matching between the kth fuzzy IF–THEN rule and the sth sample.

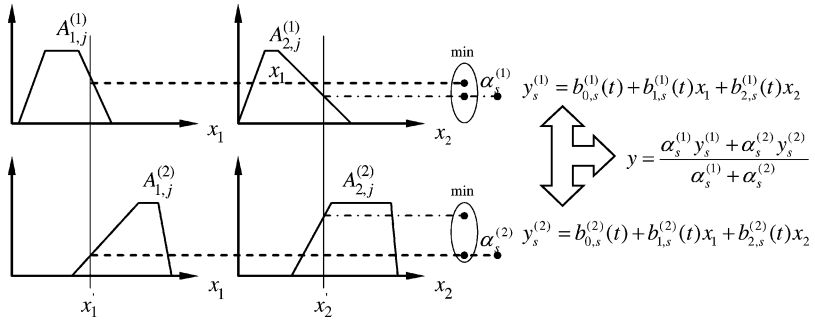

Fig. 2. TSK inference model (two-dimensional).

In this case, $N_R = 2$ and $\alpha_s^{(k)} = \min\{\mu_{A_{1,j}^{(k)}}(x_1'), \mu_{A_{2,j}^{(k)}}(x_2')\}$. The inputs to a TSK model are crisp (nonfuzzy) numbers. Therefore, the degree of input $x_1 = x_1', \ldots, x_i = x_i', \ldots, x_I = x_I'$ that matches the kth rule is typically computed using the min operator given in

$$\alpha_s^{(k)} = \min\left\{\mu_{A_{1,j}^{(k)}}(x_1'), \mu_{A_{2,j}^{(k)}}(x_2'), \cdots, \mu_{A_{I,j}^{(k)}}(x_I')\right\} \quad (4)$$

or using product operator given in

$$\alpha_s^{(k)} = \mu_{A_{1,j}^{(k)}}(x_1') \times \mu_{A_{2,j}^{(k)}}(x_2') \times \cdots \times \mu_{A_{I,j}^{(k)}}(x_I'). \quad (5)$$

Fig. 2 illustrates the computation process involved in a 2-D TSK inference model.

In TSK^0-FCMAC, the real-valued parameters $b_{1,s}^{(1)}(t)$, $b_{2,s}^{(1)}(t)$, $b_{1,s}^{(2)}(t)$, and $b_{2,s}^{(2)}(t)$ are all set to zero. Fig. 3 shows a two-input TSK^0-FCMAC with 16 rules. Four membership functions are associated with each input, so the input is partitioned into 16 fuzzy subspaces. Each fuzzy subspace is governed by a fuzzy IF–THEN rule. The premise part of a rule defines a fuzzy subspace and the consequent part specifies the output within this fuzzy subspace. In this example, four fuzzy IF–THEN rules are activated for inputs x_1' and x_2' according to their respective matching degree. They are described by

$$\begin{aligned} R_{13}&: \text{IF } x_1 \text{ is } A_{1,1}^{(13)} \text{ and } x_2 \text{ is } A_{2,3}^{(13)}, \\ &\text{THEN } y_s^{(13)}(t) = b_{0,s}^{(13)}(t) \\ R_{14}&: \text{IF } x_1 \text{ is } A_{1,1}^{(14)} \text{ and } x_2 \text{is} A_{2,4}^{(14)}, \\ &\text{THEN } y_s^{(14)}(t) = b_{0,s}^{(14)}(t) \\ R_{23}&: \text{IF } x_1 \text{ is } A_{1,2}^{(23)} \text{ and } x_2 \text{ is } A_{2,3}^{(23)}, \\ &\text{THEN } y_s^{(23)}(t) = b_{0,s}^{(23)}(t) \end{aligned}$$

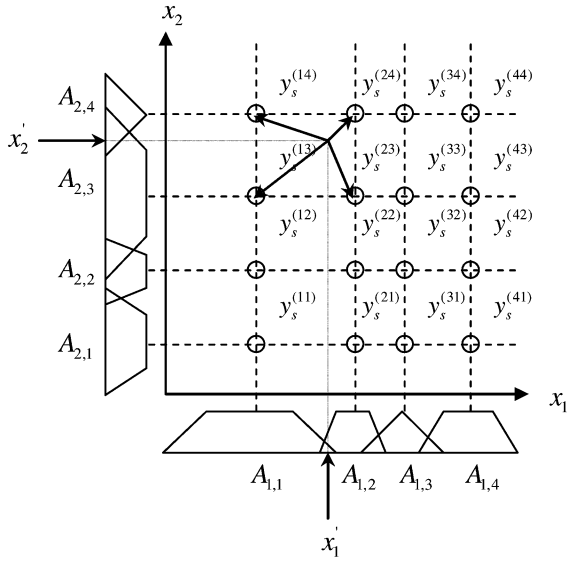

Fig. 3. Structure of two-input TSK^0-FCMAC with 16 rules.

$$\begin{aligned} R_{24}&: \text{IF } x_1 \text{ is } A_{1,2}^{(24)} \text{ and } x_2 \text{ is } A_{2,4}^{(24)}, \\ &\text{THEN } y_s^{(24)}(t) = b_{0,s}^{(24)}(t) \end{aligned} \quad (6)$$

Hence, the final output of the network is

$$y_s(t) = \frac{\alpha_s^{(13)} b_{0,s}^{(13)}(t) + \alpha_s^{(14)} b_{0,s}^{(14)}(t) + \alpha_s^{(23)} b_{0,s}^{(23)}(t) + \alpha_s^{(24)} b_{0,s}^{(24)}(t)}{\alpha_s^{(13)} + \alpha_s^{(14)} + \alpha_s^{(23)} + \alpha_s^{(24)}} \quad (7)$$

where matching degree $\alpha_s^{(k)} = \min\{\mu_{A_{1,j}^{(k)}}(x_1'), \mu_{A_{2,j}^{(k)}}(x_2')\}$.

2) Learning Algorithm: TSK^0-FCMAC employs a two-phase training algorithm. During the first phase, the DIC

$$\begin{aligned} y_s(t) &= \frac{\sum_{k=1}^{N_R} \alpha_s^{(k)} f^{(k)}(x_1, x_2)}{\sum_{k=1}^{K} \alpha_s^{(k)}} \\ &= \frac{\left[\alpha_s^{(1)}\left(b_{0,s}^{(1)}(t) + b_{1,s}^{(1)}(t)x_1 + b_{2,s}^{(1)}(t)x_2\right) + \alpha_s^{(2)}\left(b_{0,s}^{(2)}(t) + b_{1,s}^{(2)}(t)x_1 + b_{2,s}^{(2)}(t)x_2\right)\right]}{\alpha_s^{(1)} + \alpha_s^{(2)}} \end{aligned} \quad (3)$$

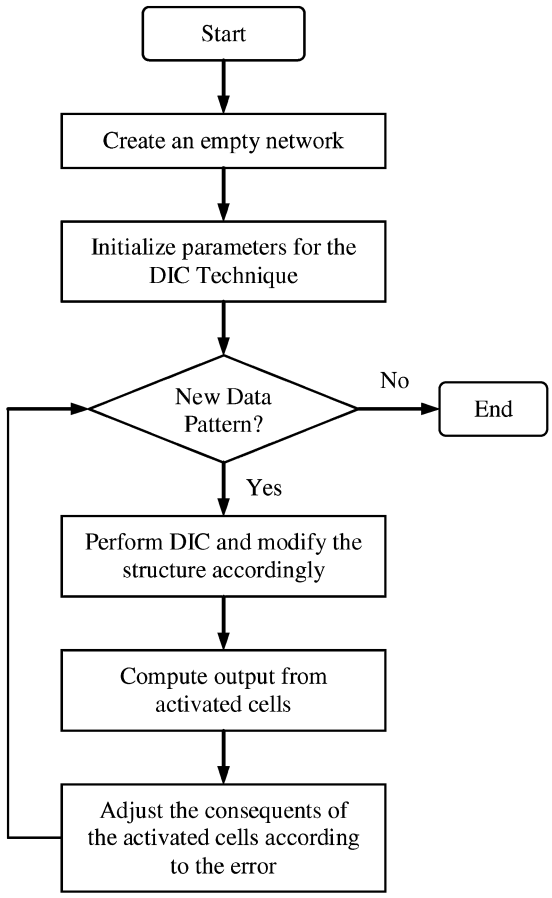

Fig. 4. Overall learning procedure.

technique [27] is performed on newly arrived data point. Depending on the degree of matching between the data point and existing clusters, DIC will create a new cluster, expand existing cluster, or do nothing. In the second phase, the same data point will activate the fuzzy IF–THEN rules within TSK^0-FCMAC and an output is computed as (7). The crisp consequents $b_{0,s}^{(k)}(t)$ for every activated fuzzy IF–THEN rule are updated as

$$b_{0,s}^{(k)}(t+1) = b_{0,s}^{(k)}(t) + \lambda \alpha_s^{(k)} \left[\hat{y}_s(t) - y_s(t)\right] \tag{8}$$

where λ is the learning parameter; $\alpha_s^{(k)}$ is the degree of matching between the kth fuzzy IF–THEN rule and the sth sample; $y_s(t)$ is the output of the network for the sth sample at the tth iteration; and $\hat{y}_s(t)$ is the target output of the network for the sth sample at the tth iteration.

The overall learning procedure is depicted in Fig. 4.

The incremental learning process of the proposed architecture is shown in Fig. 5. Initially, TSK^0-FCMAC starts with an empty structure shown in Fig. 5(a). When a new data point arrives, TSK^0-FCMAC will create a new cluster to accommodate the new data point, expand an existing cluster to include the data point, or do nothing on the existing structure (i.e. the data point falls into an existing cluster) according to the DIC technique; see Fig. 5(b) and (c). The details of the DIC technique are described in the next section.

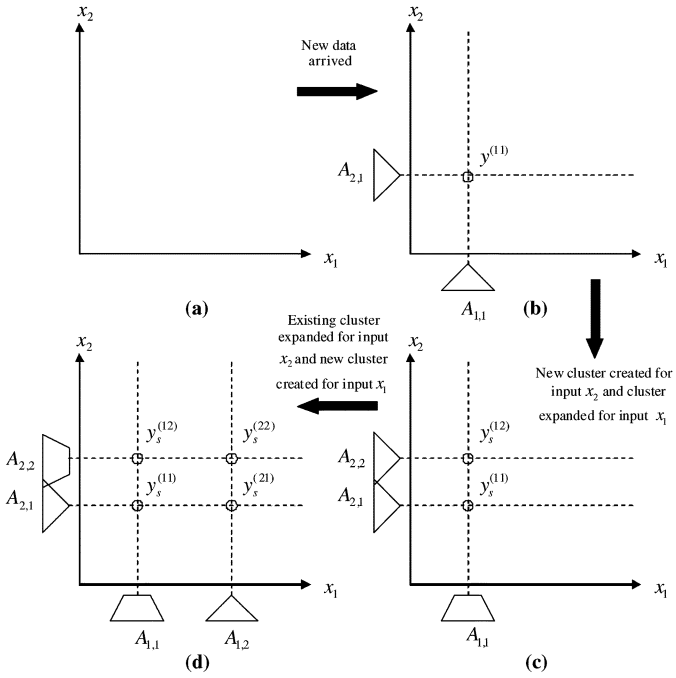

Fig. 5. TSK^0-FCMAC structure at: (a) empty; (b) after first data points; (c) after second data point; and (d) after third data point.

3) DIC Technique: Traditional clustering techniques suffer from the stability–plasticity dilemma [36], where new information cannot be learned without running the risk of eroding previously learned but valid knowledge. Therefore, neural fuzzy system such as pseudo-outer-product-based fuzzy neural network (POPFNN) [37] violates the networks' ability to self-organize and self-adapt with changing environments. Another shortcoming of these clustering techniques is the requirement of prior knowledge such as the number of classes.

In TSK^0-FCMAC, the formation of input clusters (receptive field function) is governed by a novel DIC technique proposed by Tung and Quek [27]. The DIC technique is not limited by the need to have prior knowledge of the number of clusters C and it preserves the dynamism to learn new knowledge. This novel clustering technique attempts to integrate the merits of fuzzy adaptive resonance theory (fuzzy ART) [38] and learning vector quantization (LVQ) [39] clustering techniques.

The DIC technique has five parameters: a plasticity parameter β, a tendency parameter TD, an input threshold IT, an output threshold OT and a fuzzy set support parameter SLOPE. A brief description of DIC is given in this section and full details can be found in [27].

Each new cluster in DIC begins as a triangular fuzzy set as shown in Fig. 6(a). The kernel of a new cluster (fuzzy set) takes the value of the data point (x') that triggers its creation.

As training continues, the cluster "grows" to include more points, but maintains the same amount of buffer regions on both sides of the kernel as shown in Fig. 6(b). An additional parameter STEP gradually reduces the amount of expansion for the kernel as the cluster grows.

The following algorithm performs clustering of the input space.

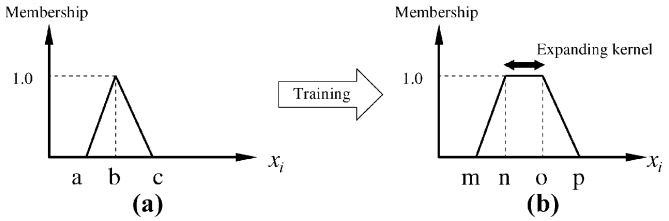

Fig. 6. (a) A newly created cluster and (b) cluster after training.

TABLE I
PATIENT A'S PROFILE

Sex	Male
Age	40 years old
Weight	70 kg
Height	174.5 cm
Body Mass Index	23
Activity Factor	Light exercise or sports 1-3 days a week
Daily Calorie Needed	1957 kcal
Corresponding Daily Carbohydrate Intake	279 grams

Algorithm DIC

Assume data set $\overline{X} = \{X^{(1)}, \ldots, X^{(p)}, \ldots, X^{(P)}\}$.

Initialize STEP, SLOPE, IT and TD.

Vector $X^{(p)} = \{X_1^{(p)}, \ldots, X_i^{(p)}, \ldots, X_I^{(p)}\}$ represents the pth input training vector to TSK^0-FCMAC.

Variable J_i represents the total number of clusters created for input x_i.

$\forall p \in \{1 \ldots P\}$

$\forall i \in \{1 \ldots I\}$

When J_i is zero, create a new cluster using $X_i^{(p)}$.

Otherwise

Determine best-fit cluster Winner such that

$$\text{Winner} = \arg \max_{j \in \{1 \ldots J_i\}} \left\{ \mu_{A_{i,j}} \left(X_i^{(p)} \right) \right\}$$

Update the kernel of the Winner if $\mu_{A_{i,\text{Winner}}}(X_i^{(p)}) >$ IT

Otherwise, create a new cluster using $X_i^{(p)}$.

End DIC.

4) Controller's Error: In the learning algorithm, the network is updated based on the difference between the desired output and the actual network output. However, in the context of blood glucose regulation, no specific desired output is available as the regulation of blood glucose in response to disturbance of food intake is constrained by the desired upper and lower bounds. As a result, a different error is devised for its learning. The statement below describes the phenomenon in blood glucose regulation:

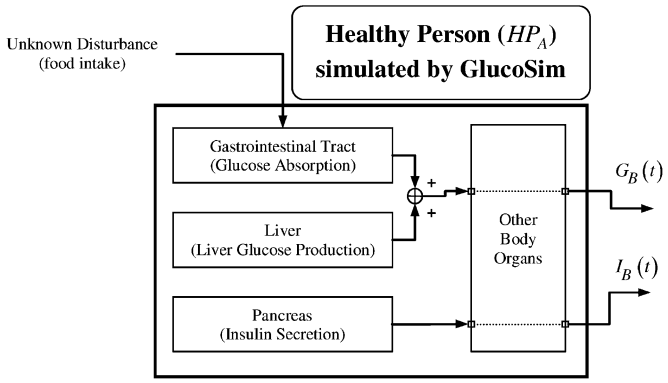

Fig. 7. Block diagram for healthy person (HP_A). $G_B(t)$ represents the actual plasma glucose level; $I_B(t)$ represents the actual plasma insulin level.

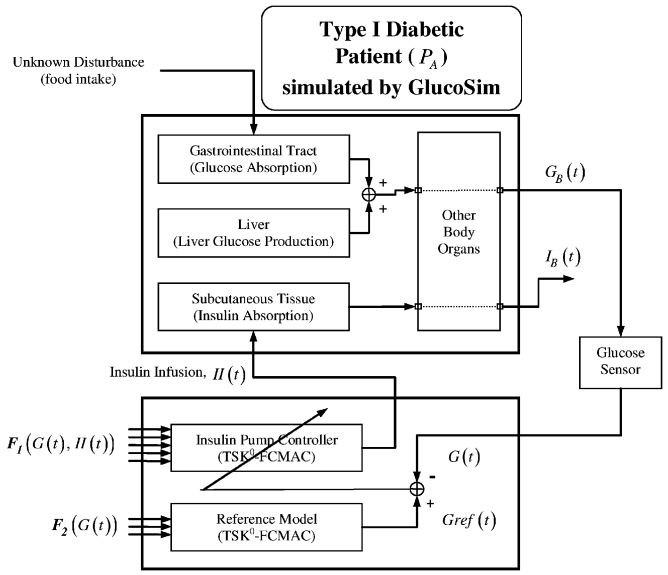

Fig. 8. Block diagram for type I diabetic patients (P_A) under closed-loop blood glucose control system. $G_B(t)$ represents the actual plasma glucose level; $G(t)$ represents the output from the glucose sensor; $\text{Gref}(t)$ represents the output from the reference model; $I_B(t)$ represents the actual plasma insulin level; $II(t)$ represents the insulin infusion rate of the insulin pump; $\mathtt{F}_1(G(t), II(t))$ represents the inputs of the controller and they are derived from historical values of $G(t)$ and $II(t)$; $\mathtt{F}_2(G(t))$ represents the inputs of the reference model and they are derived from historical readings of $G(t)$.

"Insulin delivered at time t reduces the blood glucose level at time $(t+1), (t+2), \ldots (t+n)$."

Therefore, to realize the statement above, updating cells that are activated during the current iterations alone is insufficient. Instead, the controller in our system will also update the cells that are activated previously. The error $\text{Error}_{\text{controller}}(t)$ for these updates is defined in

$$\text{Error}_{\text{controller}}(t) = (II_{\max} - II_{\min}) \times \delta_{\text{controller}} \times \frac{G(t) - \text{Gref}(t)}{\text{Gref}_{\max} - \text{Gref}_{\min}} \times \text{decay rate} \quad (9)$$

$$\text{decay rate} = -\log_{10}(0.1 + \omega \times \text{hist}) \quad (10)$$

where $II_{\max}$ and $II_{\min}$ are the maximum and minimum infusion rate for insulin pump; $\delta_{\text{controller}}$ is the learning parameter

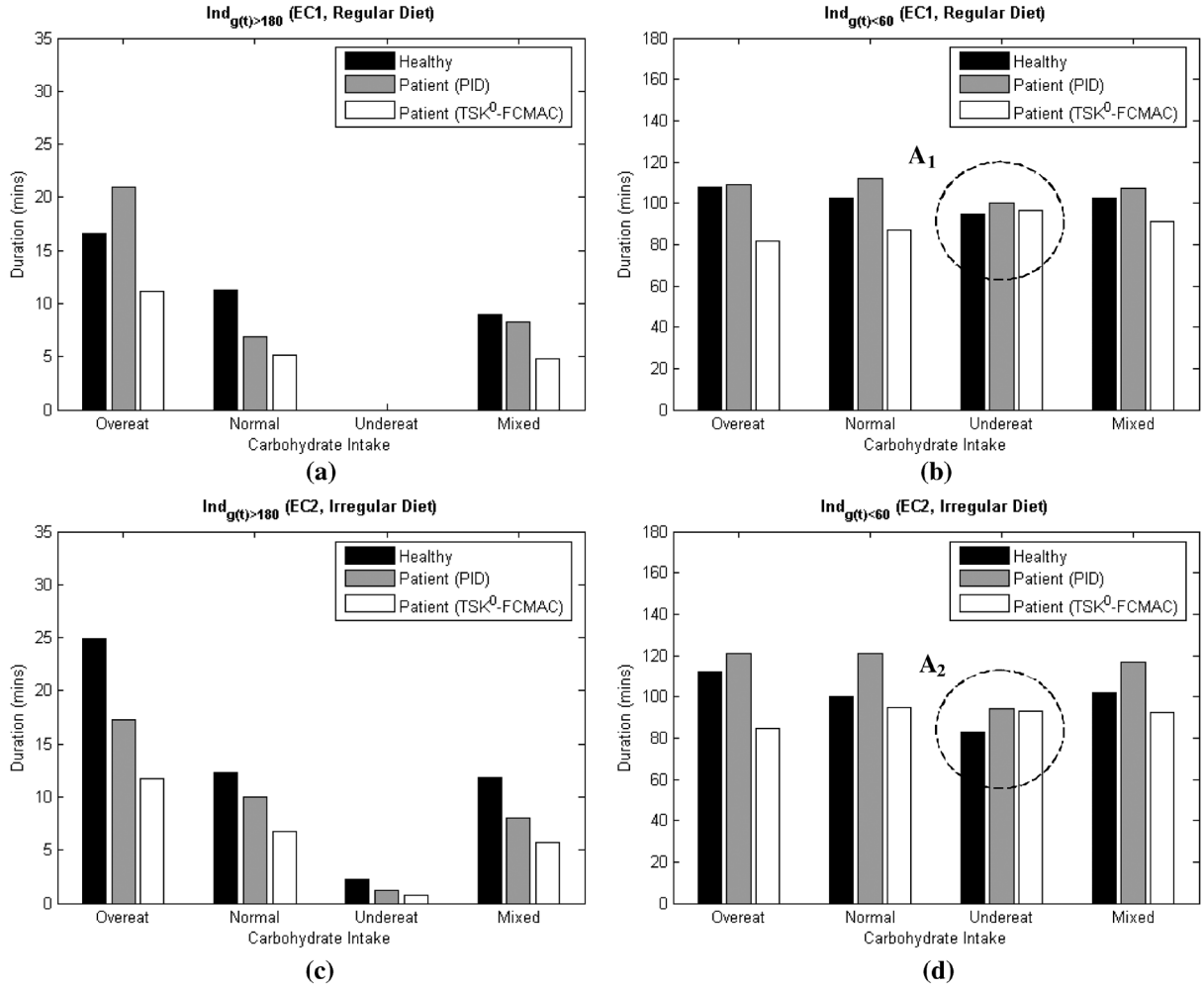

Fig. 9. Results for EC_1 and EC_2 (70 kg).

TABLE II
NOMENCLATURE

P_A	Type I diabetic patient A;
HP_A	Healthy person A. HP_A is the same as P_A except HP_A is able to regulate his own blood glucose level;
$diet_{P_A,\,CI,\,EH}$	Dietary profile of P_A with carbohydrate intake CI and eating habit EH, where $CI \in \{normal, overeat, undereat, mixed\}$ and $EH \in \{regular, irregular\}$;
$diet_{P_A,\,normal,\,EH}$	Daily carbohydrates intake equals to the amount computed based on Harris-Benedict equation [42] for P_A;
$diet_{P_A,\,overeat,\,EH}$	Daily carbohydrates intake equals to 150% of $diet_{P_A,\,normal,\,EH}$;
$diet_{P_A,\,undereat,\,EH}$	Daily carbohydrates intake equals to 50% of $diet_{P_A,\,normal,\,EH}$;
$diet_{P_A,\,mixed,\,EH}$	Daily carbohydrates intake switches among $diet_{P_A,\,normal,\,EH}$, $diet_{P_A,\,overheat,\,EH}$ and $diet_{P_A,\,underheat,\,EH}$;
$diet_{P_A,\,CI,\,regular}$	Carbohydrates intake and meal time is consistent every meal;
$diet_{P_A,\,CI,\,irregular}$	Carbohydrates intake varies between $\pm 50\%$ of the original value. Meal time varies between ± 1 hour.

TABLE III
REGULAR DIETARY PROFILE

Meal Type	Meal Time	% of Carbohyrate w.r.t. Total Carbohydrate Intake
Breakfast	0800 hrs	20%
Lunch	1200 hrs	30%
Tea break	1530 hrs	10%
Dinner	1930 hrs	40%

for controller (it is set to 0.2 to prevent drastic update on the controller's surface); $G(t)$ is the output from the glucose sensor at time t; $G\mathrm{ref}_{\max}$ and $G\mathrm{ref}_{\min}$ are the maximum and minimum allowable output from the reference model; ω is the decay constant for difference between iterations; hist is the iteration difference between current iterations and the instance when the updating cells are activated previously; and $\mathrm{hist} \in \{0, 1, 2, \ldots\}$.

III. EXPERIMENTS

This section describes how the experiments are conducted.

A. Assumptions

Many researchers developed system that requires information on food intake. The accuracy of such information is highly de-

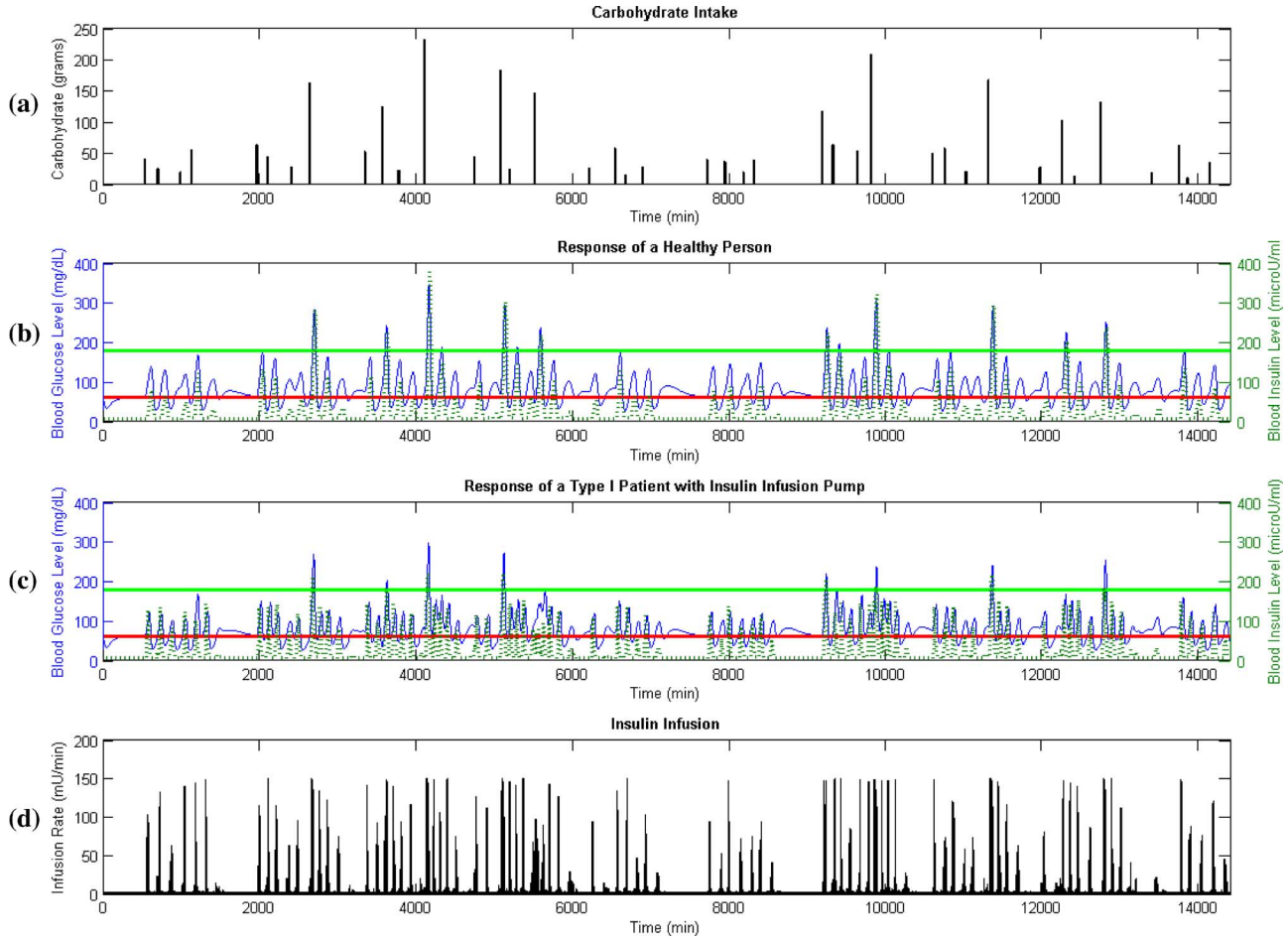

Fig. 10. Ten-day response of HP_A and P_A (with TSK^0-FCMAC controlled insulin infusion pump) under dietary profile $\mathrm{diet}_{P_A,\mathrm{mixed,irregular}}$.

pendent on the self-discipline of a patient and is susceptible to mistakes, especially for adolescent patients. The assumptions in our proposed system eliminate such needs. With the goal of possible human/animal pilot testing in mind, the following assumptions have been made prior to the conduct of the experiments.

- The blood glucose level is measured at 5-min interval, which is achievable with existing glucose monitoring devices [4].
- No measurement is available for blood insulin level.
- Dietary profile of individual is unknown.

B. Controller's Objective and Performance Indicator

The Diabetes Control and Complications Trial (DCCT) [40], a clinical study conducted by National Institute of Diabetes and Digestive and Kidney Diseases (NIDDK, USA) [41] showed that keeping blood glucose levels as close to normal as possible slows the onset and progression of eye, kidney, and nerve diseases caused by diabetes. As a result, the controller's objective is to maintain the blood glucose level at euglycemia (60 $\sim$ 110 mg/dL) before meals and $<$180 mg/dL after meals.

Two performance indicators are used to evaluate the performance of the controller. These performance indicators are defined to measure the occurrences of prolonged low and high blood glucose levels, which may lead to hypoglycemia and hyperglycemia. They describe the average duration (in terms of minutes) of blood glucose level that exceeds the condition for every diet taken by the person. They are depicted in the following:

TABLE IV
IRREGULAR DIETARY PROFILE

Meal Type	Meal Time	% of Carbohyrate w.r.t. Total Carbohydrate Intake
Breakfast	0700 hrs ~ 0900 hrs	10% : 30%
Lunch	1100 hrs ~ 1300 hrs	15% : 45%
Tea break	1430 hrs ~ 1630 hrs	5% : 15%
Dinner	1830 hrs ~ 2030 hrs	20% : 60%

- average duration of hyperglycemia

$$\mathrm{Ind}_{G(t)>180} = \frac{N_{G(t)>180}}{N_{\text{food intake}}} \times T_{\text{sampling}}; \tag{11}$$

- average duration of hypoglycemia

$$\mathrm{Ind}_{G(t)<60} = \frac{N_{G(t)<60}}{N_{\text{food intake}}} \times T_{\text{sampling}}; \tag{12}$$

where $N_{G(t)>180}$ is the total number of occurrences that the blood glucose level is above 180 mg/dL; $N_{G(t)<60}$ is the total number of occurrences that the blood glucose level is below 60 mg/dL; $N_{\text{food intake}}$ is the total number of food intakes; and

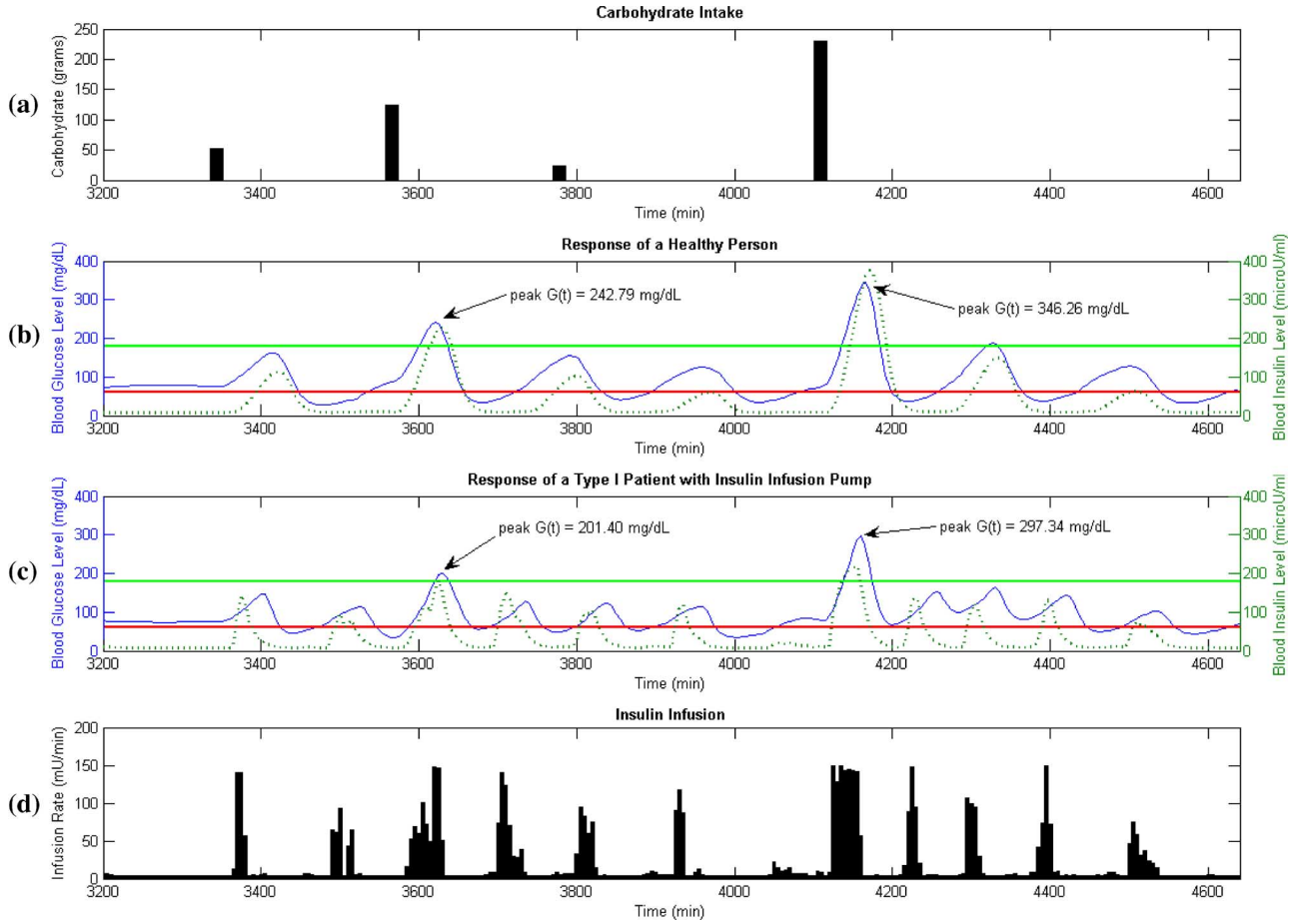

Fig. 11. Response of day 3 for HP_A and P_A (with TSK^0-FCMAC controlled insulin infusion pump) under dietary profile $diet_{P_A,mixed,irregular}$.

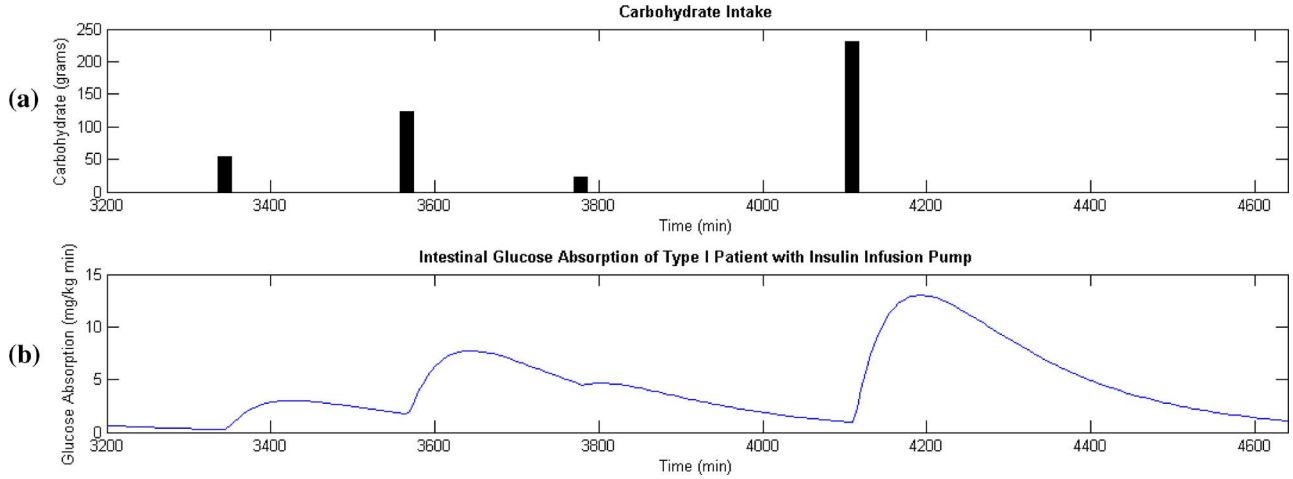

Fig. 12. Intestinal glucose absorption of day 3 for P_A (with TSK^0-FCMAC controlled insulin infusion pump) under dietary profile $\mathrm{diet}_{P_A,\mathrm{mixed},\mathrm{irregular}}$.

T_{sampling} is the duration of one iteration in the simulation. It is equal to the sampling rate of blood glucose level (5 min).

C. Simulation Setup

In order to conduct the simulation, the patient's profile and its dietary habit must be properly defined. A type I diabetic patient's profile (P_A) is formulated in our simulations and is shown in Table I. The patient is assumed to be a middle-aged Asian office worker whose job is clerical in nature. The body mass index (BMI) for the patient is set at 23 and the daily calorie intake needed is computed based on Harris–Benedict equation [42]. The computation for the corresponding daily carbohydrate intake follows the assumptions below.

- The ratio of calorie obtained from diet is as follows: carbohydrate (57%), fats (30%), and protein (13%).
- The energy yield per grams is as follows: carbohydrate (4 kcal), fats (9 kcal), and protein (4 kcal).

The dietary profile for the patient is defined from two perspectives, namely, carbohydrate intake (CI) and eating habit (EH). The nomenclature is defined in Table II.

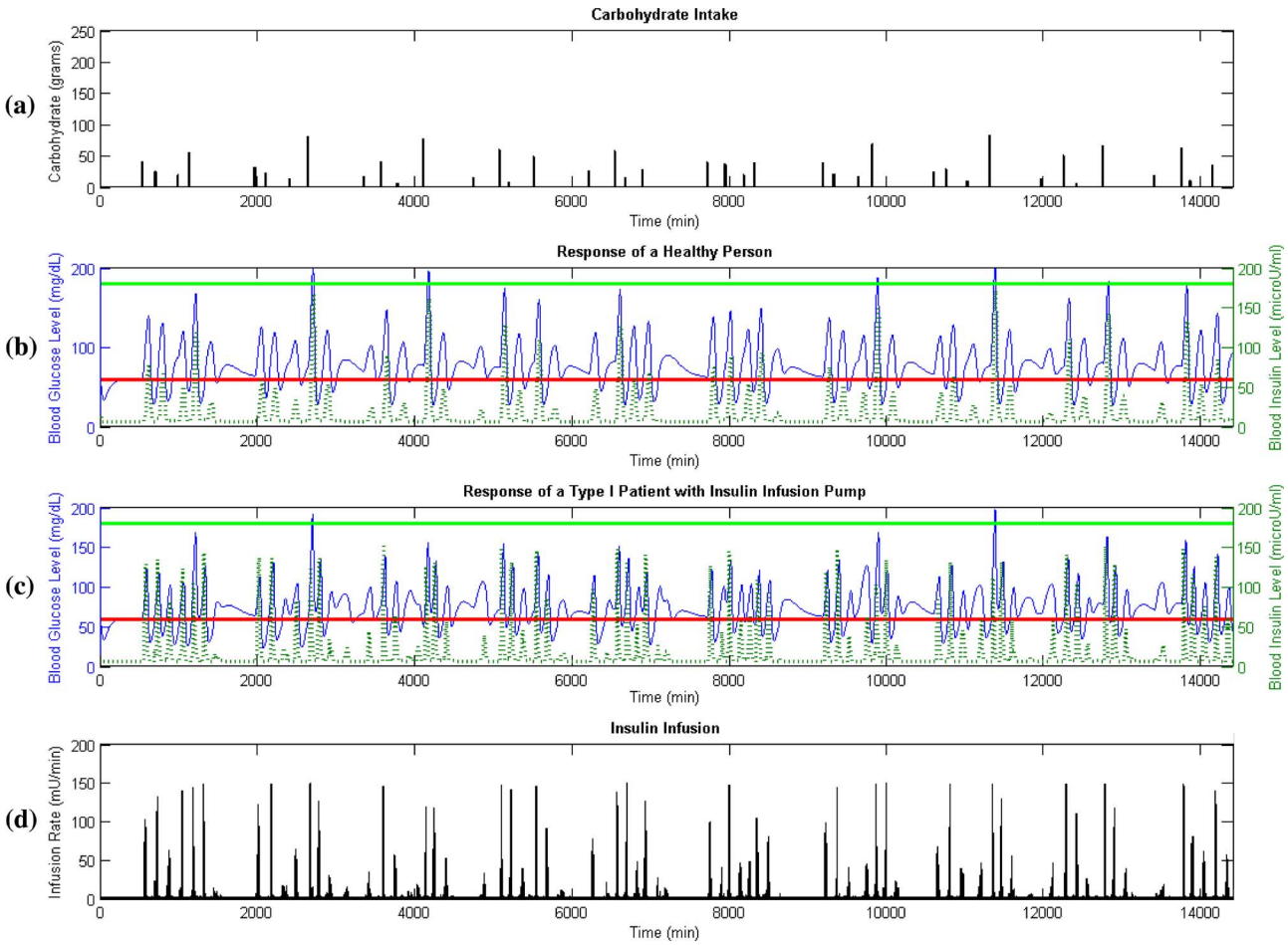

Fig. 13. Ten-day response of HP_A and P_A (with TSK^0-FCMAC controlled insulin infusion pump) under dietary profile $diet_{P_A,undereat,irregular}$.

With respect to the definitions in Table II, the dietary profiles for regular and irregular eating habit are shown as Tables III and IV.

The block diagram for a healthy person (HP_A) and type I diabetic patient (P_A) under insulin infusion pump are shown in Figs. 7 and 8, respectively. It illustrates a simplified glucose–insulin model by highlighting the gastrointestinal tract, liver, pancreas, and subcutaneous tissue only. The detailed glucose–insulin model can be found in [10] and [26]. In Fig. 8, the pancreas of the diabetic patient is replaced by subcutaneous tissue where external insulin source is supplied. In the simulation, regular insulin is supplied through an insulin infusion pump controlled by a TSK^0-FCMAC network.

D. Results and Discussion

To reduce the risk of complications from diabetic mellitus, the lifestyle of a type I diabetic patient must be under continuous scrutiny. Much of these require human interventions and are susceptible to mistakes. As a result, the proposed closed-loop control system must be able to operate with minimum human intervention. Information such as food intake should not be included as part of the input to the system. With such limitations, our goal is to implement a closed-loop blood glucose control system that is capable of handling: 1) intrapersonal variations, and 2) interpersonal variations.

The first TSK^0-FCMAC network (referred to as the reference model) was trained by modeling the simulated response of a healthy person (HP_A). The training data are collected by simulating a healthy person under irregular dietary profile with GlucoSim. It is responsible to provide reference blood glucose level for the controller of the insulin infusion pump. The trained reference model is a three-inputs TSK^0-FCMAC network with the size of 18 cells $(3\times2\times3)$. The inputs of the network are derived from historical reading of the glucose sensor $(G(t))$. The three inputs are represented in the form of $\{x_1(t), x_2(t), x_3(t)\}$ and are computed as

$$x_1(t) = G_1(t) \tag{13}$$

$$x_2(t) = \begin{cases} \text{sign}\left(G_{1,4}(t)\right)\ln\left(|G_{1,4}(t)|\right), & \text{if } |G_{1,4}(t)| \le 1 \\ 0, & \text{otherwise} \end{cases} \tag{14}$$

$$x_3(t) = \begin{cases} \text{sign}\left(H_{1,4}(t)\right)\ln\left(|H_{1,4}(t)|\right), & \text{if } |H_{1,4}(t)| \le 1 \\ 0, & \text{otherwise} \end{cases} \tag{15}$$

$$G_i(t) = G(t - i \times T_{\text{sampling}}) \tag{16}$$

$$G_{i,j}(t) = G_i(t) - G_j(t) \tag{17}$$

$$H_{i,j}(t) = G_{i,j}(t) - G_{i,j}(t - T_{\text{sampling}}) \tag{18}$$

where $G(t)$ is the output from the glucose sensor at time t; T_{sampling} is the duration of one iteration in the simulation [it

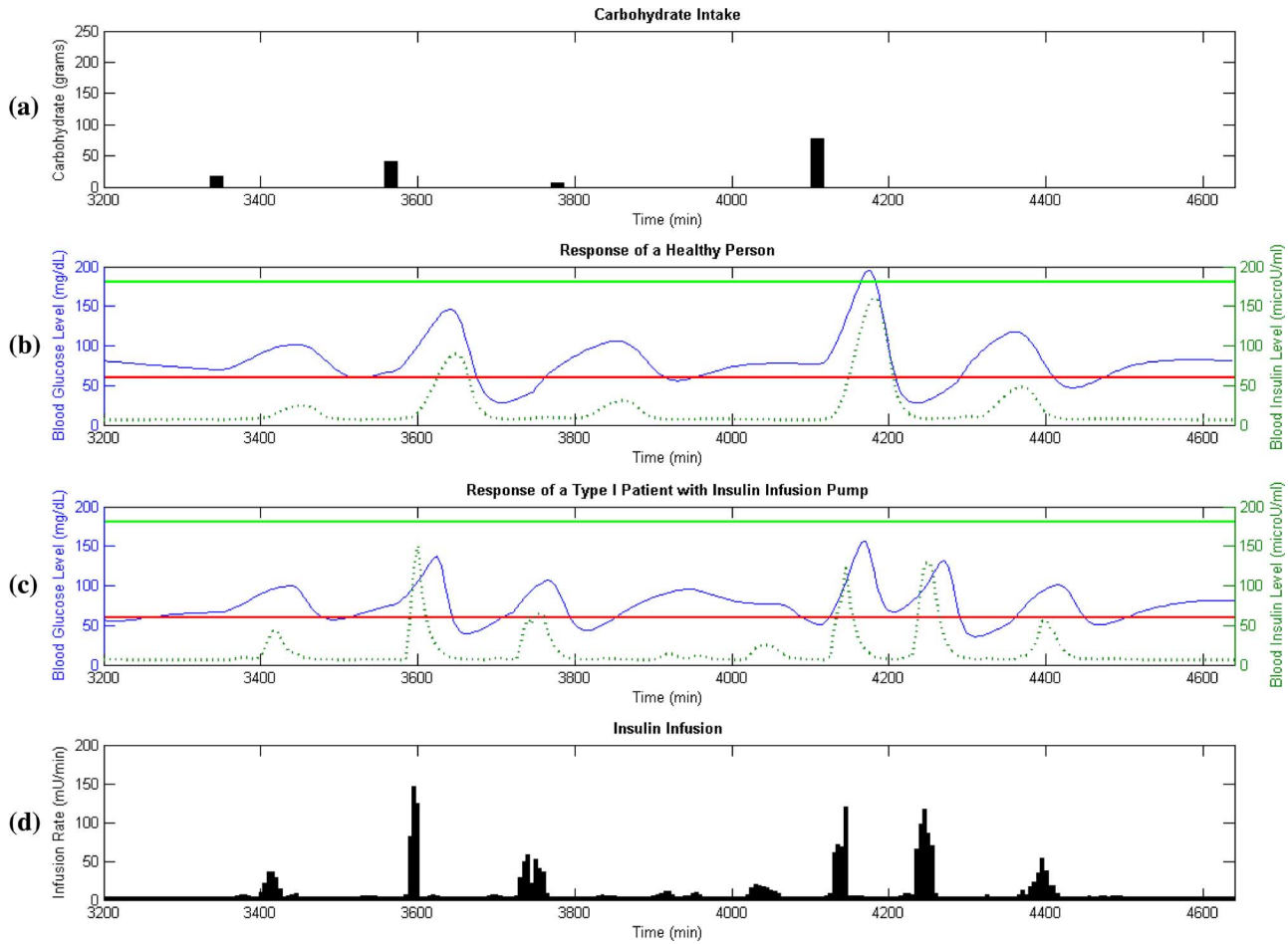

Fig. 14. Response of day 3 for HP_A and P_A (with TSK^0-FCMAC controlled insulin infusion pump) under dietary profile $\mathrm{diet}_{P_A,\mathrm{undereat},\mathrm{irregular}}$.

is equal to the sampling rate of blood glucose level (5 min)]; and $\mathrm{sign}(.)$ is the function that returns the sign value.

A second TSK^0-FCMAC network (referred to as the TSK^0-FCMAC controller), was subsequently trained to control the infusion rate for insulin infusion pump. As shown in Fig. 8, the reference model and the controller were attached to a type I diabetic patient (P_A). The controller started as an empty TSK^0-FCMAC network. As shown in Fig. 5, input clusters were formed and trained online as new data arrived. Irregular diet was supplied to the patient P_A to cover the whole spectrum of his eating habit. The trained controller is a five-input fuzzy CMAC network with the size of 13 440 cells $(8\times8\times7\times6\times5)$, which is equivalent to 13 440 fuzzy IF–THEN rules of TSK's type [24], [25]. Out of these rules, a total of 1761 rules are trained. The utilization ratio of the TSK^0-FCMAC network is hence equal to $1761/13440 = 13.1\%$. This utilization ratio is deemed as passable considering that the controller is trained to cover the whole spectrum of a patient's eating habit. The inputs of the network are derived from historical reading of the glucose sensor $(G(t))$ and the previous insulin infusion rate $(II(t))$. The five inputs are represented in the form of $\{x_1(t), x_2(t), x_3(t), x_4(t), x_5(t)\}$. The first three inputs are the same as the inputs employed by the reference model (i.e., the first TSK^0-FCMAC network) and the last two inputs are computed as

$$x_4(t) = \frac{\sum_{i=1}^{12} G_i(t)}{12} \tag{19}$$

$$x_5(t) = \frac{\sum_{i=1}^{12} II_i(t)}{12} \tag{20}$$

$$II_i(t) = II(t - i \times T_{\mathrm{sampling}}) \tag{21}$$

where $II(t)$ is the infusion rate for insulin pump at time t.

The performance of the proposed system is compared with a PID controller. Conventional tuning method such as the Ziegler–Nichols method [43] involves investigating the step response of the plant (i.e., human subject in this case), which may not present a viable approach in clinical trial on live human subject. This implies that the glucose reference is to be toggled, and controlled response is observed. Such an exogenous probe signal would be considered clinically intrusive and would be difficult to clear the biomedical ethics board. As such we have not pursued this approach given the clinical reservation. Hence, the parameters of the PID controller are tuned manually. The need for manual tuning also draws the attention to the short-

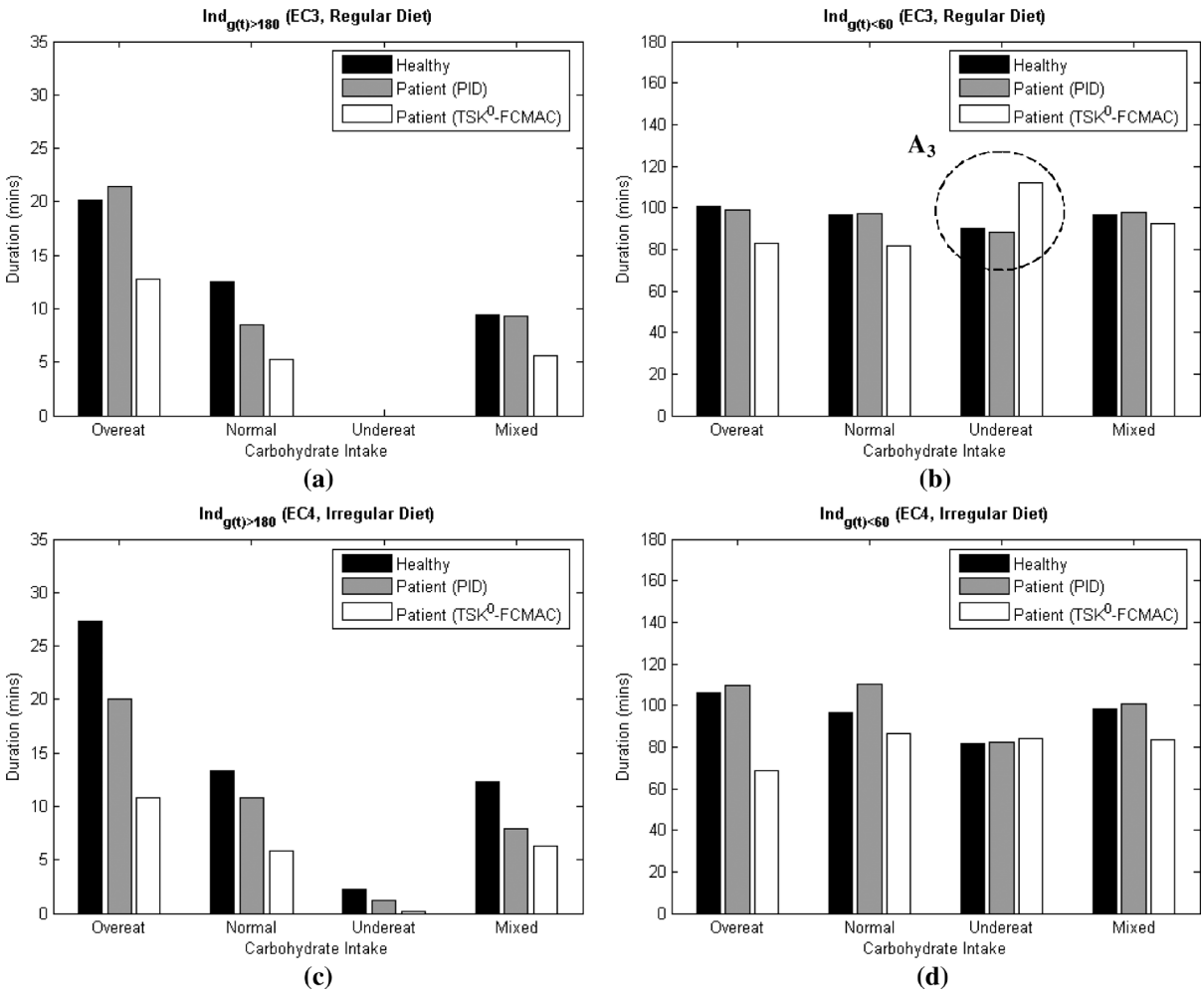

Fig. 15. Results for EC_3 and EC_4 (73.5 kg).

coming of having a PID controller designed in offline approach. The infusion rate of the PID controller is computed as

$$\begin{aligned} II(t) = & K_p \times \mathrm{Error}_{\mathrm{PID}}(t - T_{\mathrm{sampling}}) \\ & + K_i \times \int_{t-T_{\mathrm{sampling}}}^{t-12\times T_{\mathrm{sampling}}} \mathrm{Error}_{\mathrm{PID}}(\tau) d\tau \\ & + K_d \times \begin{bmatrix} \mathrm{Error}_{\mathrm{PID}}(t - T_{\mathrm{sampling}}) \\ -\mathrm{Error}_{\mathrm{PID}}(t - 2 \times T_{\mathrm{sampling}}) \end{bmatrix} \end{aligned} \tag{22}$$

$$\mathrm{Error}_{\mathrm{PID}}(t) = G(t) - G\mathrm{ref} \tag{23}$$

where K_p is the proportional gain of the PID controller $K_p = 140$; K_i is the integral gain of the PID controller $K_i = -10$; K_d is the derivative gain of the PID controller $K_d = 140$; T_{sampling} is the duration of one iteration in the simulation [it is equal to the sampling rate of blood glucose level (5 min)]; and $G\mathrm{ref}$ is the set point of the PID controller $G\mathrm{ref} = 110.0$;

With the trained controllers (both the TSK^0-FCMAC controller and the PID controller), experimental cases are formulated to examine the controllers' ability in handling intra- and interpersonal variations. Each experimental case consists of 40 diets within the ten-day simulation. The same diets are simulated on both a healthy person (HP_A) and a type I diabetic patient (P_A) for comparison. The block diagrams are shown in Figs. 7 and 8, respectively.

1) Intrapersonal Variation: Individual tends to change his dietary habit. A rigid system that assumes a fixed regular diet may not be able to handle such situations. As a result, the first two experimental cases are designed to examine the ability of the proposed system in handling intrapersonal variations. The same controller is used to control the insulin infusion rate of the same patient under different dietary profile. The experimental cases are listed as follows.

- Case 1: EC_1: apply the trained controllers on P_A with regular eating habit $\mathrm{diet}_{P_A,CI,\mathrm{regular}}$;
- Case 2: EC_2: apply the trained controllers on P_A with irregular eating habit $\mathrm{diet}_{P_A,CI,\mathrm{irregular}}$;

where $CI \in \{\mathrm{normal}, \mathrm{overeat}, \mathrm{undereat}, \mathrm{mixed}\}$.

Fig. 9 presents the results for EC_1 and EC_2. The performance of a healthy person is represented in black. The performance of a type I diabetic patient with PID controlled insulin infusion pump is represented in gray. The performance of a type I diabetic patient with TSK^0-FCMAC controlled insulin infusion pump is represented in white.

From the bar charts, it can be noticed that the TSK^0-FCMAC controller (white colored bar) is able to achieve a significantly shorter period of hyperglycemia $(\mathrm{Ind}_{G(t)>180})$ for all dietary

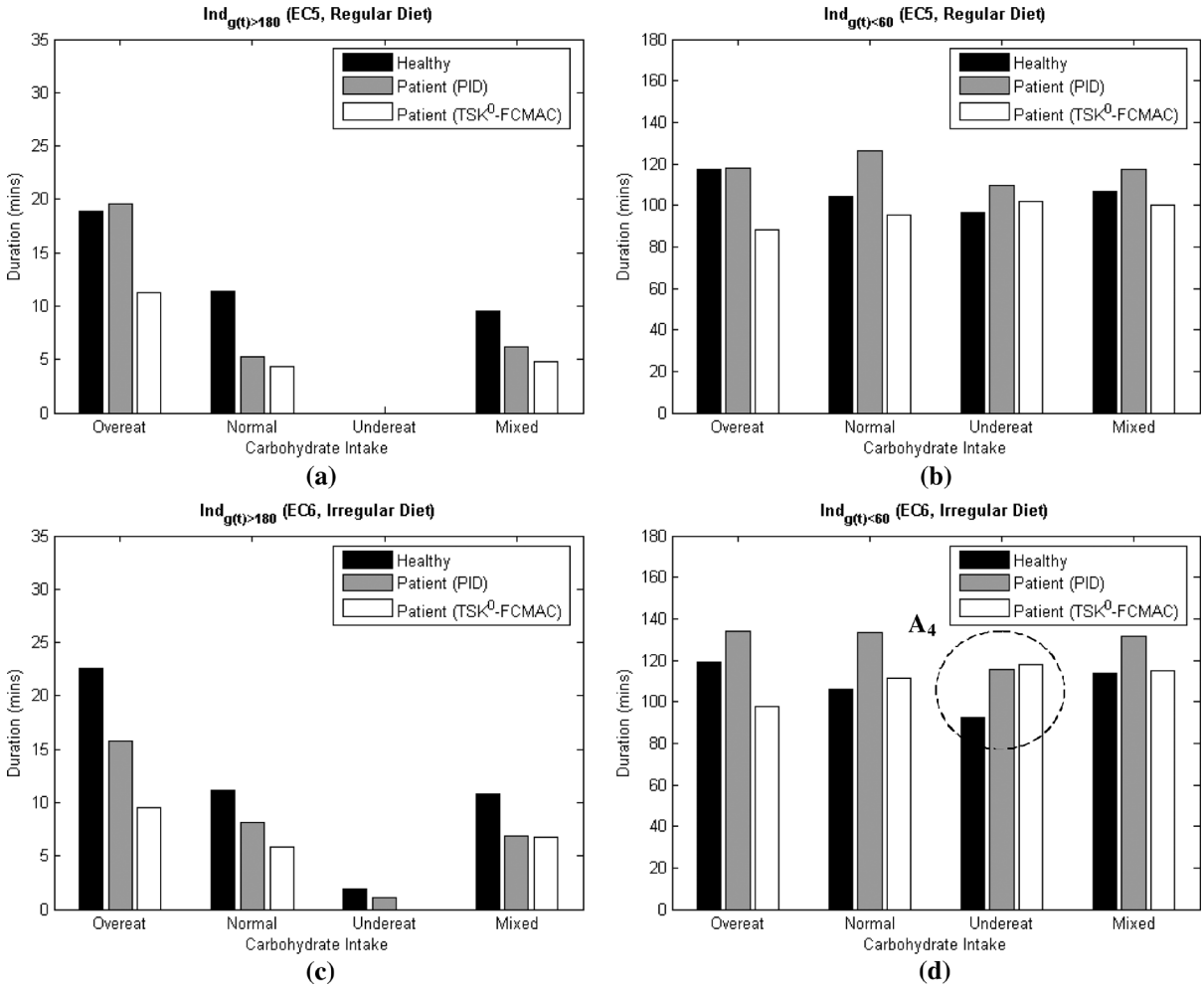

Fig. 16. Results for EC_5 and EC_6 (66.5 kg).

profiles [as shown in Fig. 9(a) and (c)]. On the other hand, there is only a slightly longer period of hypoglycemia $(\mathrm{Ind}_{G(t)<60})$ when the patient is under dietary profile of under eating [as highlighted by A_1 and A_2 in Fig. 9(b) and (d)]. In addition, the duration of hyperglycemia and hypoglycemia in a patient with TSK^0-FCMAC controlled insulin infusion pump is notably shorter than that of PID controlled in all cases.

Fig. 10 shows the ten-day simulated results for HP_A and P_A (with TSK^0-FCMAC controlled insulin infusion pump) under the same dietary profile $\mathrm{diet}_{P_A,\mathrm{mixed,irregular}}$. Fig. 10(a) shows their carbohydrates intake. Fig. 10(b) and (c) shows the respective simulated response of HP_A and P_A under the same carbohydrates intake. The simulated blood glucose level is represented by solid line and the simulated blood insulin level is represented by dotted line. The two horizontal lines indicate the upper acceptable limit (180 mg/dL) and lower acceptable limit (60 mg/dL) for the blood glucose level. The insulin infusion rates for P_A are shown in Fig. 10(d). Fig. 10 shows that the simulated response for P_A under TSK^0-FCMAC controlled insulin infusion pump is comparable with that of a healthy person. The blood glucose level is bounded within its limit under different carbohydrate intake and meal time.

For further analysis, the simulated response of day 3 is shown in Fig. 11. Day 3 is chosen because one of its meals contains the highest carbohydrate intake over the ten-day period. The simulated blood glucose level exceeded the upper limit of 180 mg/dL in two instances due to huge amount of carbohydrate intake. As indicated in the charts, the peak of P_A (201.40 and 297.34 mg/dL) is significantly lower than that of the healthy person (242.79 and 346.26 mg/dL). The shorter duration of hyperglycemia is mainly because of the early detection of possible rising glucose level. As shown in the simulated response for P_A, the TSK^0-FCMAC controller is able to anticipate the increase of the insulin infusion rate before the rising of blood glucose level. It can also be observed that the duration of hypoglycemia in P_A is slightly shorter than that in HP_A. Another observation from Fig. 11 is that insulin infusion can still be observed several hours after food intake. The observed insulin infusion is because of the continuous

TABLE V
PATIENT B'S AND PATIENT C'S PROFILES

Patient	P_B	P_C
Weight	73.5 kg	66.5 kg
Body Mass Index	24.14	21.84
Daily Calorie Needed	2014 kcal	1899 kcal
Corresponding Daily Carbohydrate Intake	287 grams	270 grams

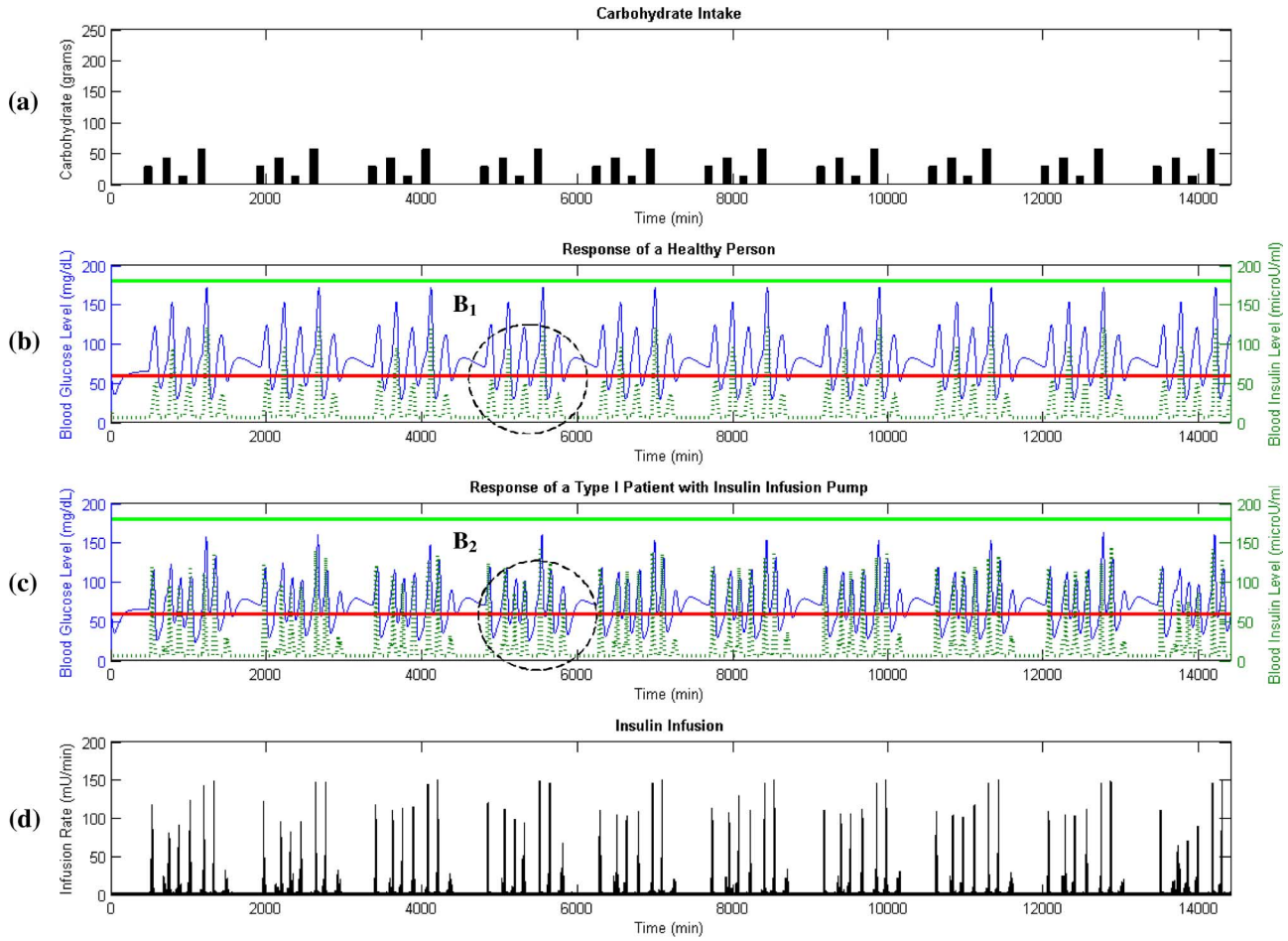

Fig. 17. Ten-day response of HP_B and P_B (with TSK^0-FCMAC controlled insulin infusion pump) under dietary profile $\mathrm{diet}_{P_B,\mathrm{undereat},\mathrm{regular}}$.

absorption of glucose in the gastrointestinal tract. Fig. 12 shows the glucose absorption in gastrointestinal tract of P_A. The absorption of glucose in gastrointestinal tract is a gradual process. This process declines progressively after food intake and it explains the needs of insulin.

As mentioned previously, the duration of hypoglycemia $(\mathrm{Ind}_{G(t)<60})$ for patient under dietary profile of $\mathrm{diet}_{P_A,\mathrm{undereat},EH}$ is slightly longer than that of a healthy person [refer to Fig. 9(b) and (d)]. As part of the analysis, the ten-day simulated response under dietary profile of $\mathrm{diet}_{P_A,\mathrm{undereat},\mathrm{irregular}}$ is shown in Fig. 13. Closer observation on a single-day response (refer to Fig. 14) suggests that the response of P_A is acceptable. The reason of higher $\mathrm{Ind}_{G(t)<60}$ is mainly because of additional occurrence (per diet) of having the glucose level decreases beyond the lower limit of 60 mg/dL. The regulation of glucose is based on the model reference paradigm However, as it can be seen in the results derived from our human pilot trials for the modeling of blood glucose/insulin at the KK Woman and Children Hospital (KKH, Singapore) for intrapatient metabolism (over a discontinuous three-day study, eight-weeks apart) [44], the healthy human glucose profile never drop below 4 mmol/l (about 54 mg/dL). Hence, this is more likely the result of the reference training model based on Glucosim. We are in the process of gathering the healthy human glucose–insulin profiles to recalibrate the intelligent schedule. Nevertheless, the duration of each occurrence is comparable with that of a healthy person and no prolonged hypoglycemic condition is detected.

As discussed previously, EC_1 and EC_2 are designed to examine the ability of the proposed system in handling intrapersonal variations. Simulated results show that the proposed TSK^0-FCMAC controller is able to handle the glucose–insulin dynamics of the same patient under all different dietary profiles.

2) Interpersonal Variation: The glucose–insulin dynamics simulated by GlucoSim [26] are average values based on individual body weight. To study interpersonal variations under the proposed control regime, two different patients P_B and P_C are formulated and are shown in Table V. They are the same as P_A except having different body weight ($\pm 5\%$).

Four additional experimental cases are designed to examine the ability of the controllers (trained for P_A) to adapt to the glucose–insulin dynamics of different patients (P_B and P_C). They are listed as follows:

- Case 3: EC_3: apply the trained controllers on P_B with regular eating habit, $\mathrm{diet}_{P_B,CI,\mathrm{regular}}$;
- Case 4: EC_4: apply the trained controllers on P_B with irregular eating habit $\mathrm{diet}_{P_B,CI,\mathrm{irregular}}$;
- Case 5: EC_5: apply the trained controllers on P_C with regular eating habit $\mathrm{diet}_{P_C,CI,\mathrm{regular}}$;
- Case 6: EC_6: apply the trained controllers on P_C with irregular eating habit $\mathrm{diet}_{P_C,CI,\mathrm{irregular}}$;

where $CI \in \{\mathrm{normal}, \mathrm{overeat}, \mathrm{undereat}, \mathrm{mixed}\}$.

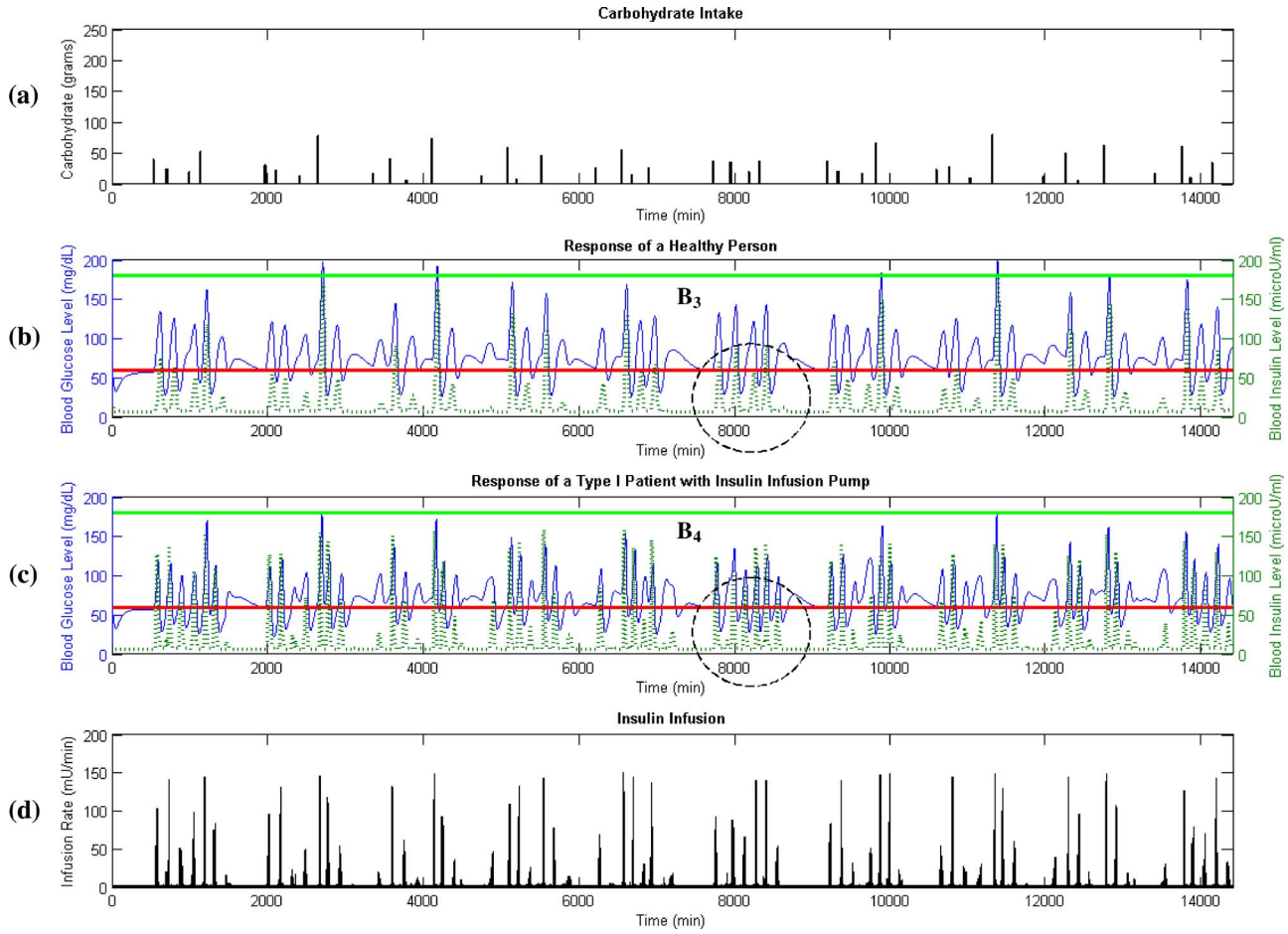

Fig. 18. Ten-day response of HP_C and P_C (with TSK^0-FCMAC controlled insulin infusion pump) under dietary profile $\mathrm{diet}_{P_C,\mathrm{undereat,irregular}}$.

Figs. 15 and 16 show the results of applying the controller trained for P_A (both the TSK^0-FCMAC controller and the PID controller) on different patients P_B and P_C. The results are analogous to those of EC_1 and EC_2 in Fig. 9. The duration of hyperglycemia $(\mathrm{Ind}_{G(t)>180})$ for diabetic patients with TSK^0-FCMAC controlled insulin infusion pump is shorter than that of the healthy person for all dietary profiles. In addition, the duration of hyperglycemia and hypoglycemia in a patient with TSK^0-FCMAC controlled insulin infusion pump is notably shorter than that of PID controlled in most cases. However, there are two cases where the duration of $\mathrm{Ind}_{G(t)<60}$ for patient (with TSK^0-FCMAC controller) is notably longer than that of a healthy person. They are as follows.

- P_B with TSK^0-FCMAC controlled insulin infusion pump (112.00 min) under dietary profile of $\mathrm{diet}_{P_B,\mathrm{undereat,regular}}$ versus HP_B (89.75 min) in EC_3 [as highlighted by A_3 of Fig. 15(b)].
- P_C with TSK^0-FCMAC controlled insulin infusion pump (118.00 min) under dietary profile of $\mathrm{diet}_{P_C,\mathrm{undereat,irregular}}$ versus HP_C (92.50 min) in EC_6 [as highlighted by A_4 of Fig. 16(d)].

For further investigation, their simulated responses over the ten-day period are presented in Figs. 17 and 18, respectively. Likewise, the higher $\mathrm{Ind}_{G(t)<60}$ is mainly due to the additional occurrence (per diet) of having the glucose level decreases beyond the lower limit. An example for such observation can be shown by comparing the regions highlighted by B_1 and B_2 in Fig. 17. There are five occurrences of having the glucose level decreased beyond the lower acceptable limit (60 mg/dL) in region B_1. However, there are six occurrences in region B_2 even though they are under the same carbohydrate intake. Similar observation is highlighted by region B_3 (four occurrences) and B_4 (six occurrences) in Fig. 18. Nevertheless, no prolonged hypoglycemic condition is detected in both cases. These results show no evidence of instability in the system even though the controller is applied on patients with different profile ($\pm 5\%$ in body weight).

IV. Conclusion

The direction for a real-life implementation of the proposed system is divided into three phases.

- Phase I: Provide a "coarse" model of artificial pancreas that is able to capture the personalized glucose–insulin dynamics of individual without meal announcement. This includes the use of mathematical model that has a close resemblance to human, that is, GlucoSim in this case. The model identified will be able to handle type I diabetic patients that is partitioned into groups with similar profile (e.g., 65–70, 70–75, and 75–80 kg).

- Phase II: Conduct medical trials on healthy human subjects under different scenarios to model the glucose–insulin dynamics of living subjects. Findings in Phase II will bestow further enhancement on the "coarse" model identified in Phase I.
- Phase III: According to the findings in Phases I and II, apply the coalesced artificial pancreas on live subjects under close scrutiny of medical practitioner.

This paper presents the investigations for Phase I, a novel blood glucose regulation for type I diabetes patient using a fuzzy CMAC-based controller. Without prior knowledge of disturbance (e.g., food intake), the proposed fuzzy CMAC is able to capture the glucose–insulin dynamics of individuals with different dietary profiles. In the simulations, the carbohydrates intake (disturbance) varies between 50% and 150% of the amount computed based on Harris–Benedict equation [42]. Preliminary simulations show that the proposed system is capable of handling both intra- and interpersonal variations. The design of the proposed system follows closely to what is available in real life and hence suitable for animal and clinical pilot testing in the following phases. Currently, medical trials for Phase II are undergoing and at the same time, the Institutional Review Board (IRB) for Phase III is under clearance for further investigations.

REFERENCES

[1] World Health Organization, Sep. 2006 [Online]. Available: http://www.who.int/mediacentre/factsheets/fs312/en/, accessed: Oct. 15, 2008.

[2] R. J. Morff, K. W. Johnson, D. Lipson, J. J. Mastrototaro, C. C. Andrew, and A. R. Potvin, "Microfabrication of reproducible, economical, electroenzymatic glucose sensors," in *Proc. 12th IEEE Annu. Int. Conf. Eng. Med. Biol. Soc.*, 1990, pp. 483–484.

[3] J. J. Mastrototaro, K. W. Johnson, D. C. Howey, P. L. Burden-Brady, R. L. Brunelle, H. M. Rowe, C. C. Andrew, B. W. Noffke, W. C. McMahan, N. A. Bryan, R. J. Morff, and D. Lipson, "Preliminary clinical results from an electroenzymatic glucose sensor implanted in subcutaneous tissue," in *Proc. 14th IEEE Annu. Int. Conf. Eng. Med. Biol. Soc.*, 1992, pp. 153–154.

[4] J. A. Tamada, M. Lesho, and M. J. Tierney, "Keeping watch on glucose," *IEEE Spectrum*, vol. 39, no. 4, pp. 52–57, Apr. 2002.

[5] R. Bergman, L. Phillips, and C. Cobelli, "Physiologic evaluation of factors controlling glucose tolerance in man," *J. Clin. Invest.*, vol. 68, pp. 1456–1467, 1981.

[6] J. R. Guyton, R. O. Foster, J. S. Soeldner, M. H. Tan, C. B. Kahn, L. Koncz, and R. E. Gleason, "A model of glucose-insulin homeostasis in man that incorporates the heterogenous fast pool theory of pancreatic insulin release," *Diabetes Care*, vol. 27, pp. 1027–1042, 1978.

[7] J. T. Sorensen, "A physiologic model of glucose metabolism in man and its use to design and assess improved insulin therapies for diabetes," Ph.D. dissertation, Dept. Chem. Eng., Massachusetts Inst. Technol., Cambridge, MA, 1985.

[8] M. Berger and D. Rodbard, "Computer simulation of plasma insulin and glucose dynamics after subcutaneous insulin injection," *Diabetes Care*, vol. 12, pp. 725–736, 1989.

[9] W. R. Puckett, "Dynamic modeling of diabetes mellitus," Ph.D. dissertation, Dept. Chem. Eng., Wisconsin-Madison University, Madison, WI, 1992.

[10] M. Eren, B. U. Agar, F. C. Erzen, and A. Cinar, "GlucoSim: A web-based educational simulation package for glucose-insulin levels in the human body," [Online]. Available: http://216.47.139.196/glucosim/index.html Accessed: Oct. 15, 2008

[11] Automated Insulin Dosage Advisor (AIDA), Mar. 1996 [Online]. Available: http://www.2aida.org/aida/, Accessed: Oct. 15, 2008

[12] F. Chee, T. Fernando, and P. V. van Heerden, "Closed-loop glucose control in critically ill patients using continuous glucose monitoring system (CGMS) in real time," *IEEE Trans. Inf. Technol. Biomed.*, vol. 7, no. 1, pp. 43–53, Mar. 2003.

[13] R. S. Parker, F. J. Doyle, III, and N. A. Peppas, "A model-based algorithm for blood glucose control in Type I diabetic patients," *IEEE Trans. Biomed. Eng.*, vol. 46, no. 2, pp. 148–157, Feb. 1999.

[14] A. Roy and R. S. Parker, "Mixed meal modeling and disturbance rejection in type I diabetic patients," in *Proc. 28th IEEE Annu. Int. Conf. Eng. Med. Biol. Soc.*, 2006, pp. 323–326.

[15] F. Chee, T. L. Fernando, A. V. Savkin, and V. van Heeden, "Expert PID control system for blood glucose control in critically ill patients," *IEEE Trans. Inf. Technol. Biomed.*, vol. 7, no. 4, pp. 419–425, Dec. 2003.

[16] F. Chee, A. V. Savkin, T. L. Fernando, and S. Nahavandi, "Optimal H-infinity insulin injection control for blood glucose regulation in diabetic patients," *IEEE Trans. Biomed. Eng.*, vol. 52, no. 10, pp. 1625–1631, Oct. 2005.

[17] K. H. Kienitz and T. Yoneyama, "A robust controller for insulin pumps based on H-infinity theory," *IEEE Trans. Biomed. Eng.*, vol. 40, no. 11, pp. 1133–1137, Nov. 1993.

[18] P. Dua, F. J. Doyle, and E. N. Pistikopoulos, "Model-based blood glucose control for type 1 diabetes via parametric programming," *IEEE Trans. Biomed. Eng.*, vol. 53, no. 8, pp. 1478–1491, Aug. 2006.

[19] V. Tresp, T. Briegel, and J. Moody, "Neural-network models for the blood glucose metabolism of a diabetic," *IEEE Trans. Neural Netw.*, vol. 10, no. 5, pp. 1204–1213, Sep. 1999.

[20] F. Andrianasy and M. Milgram, "Applying neural networks to adjust insulin-pump doses," in *Proc. IEEE Workshop Neural Netw. Signal Process.*, 1997, pp. 182–188.

[21] M. F. Alamaireh, "A predictive neural network control approach in diabetes management by insulin administration," in *Proc. Int. Conf. Inf. Commun. Technol.*, 2006, pp. 1618–1623.

[22] S. G. Mougiakakou, K. Prountzou, and K. S. Nikita, "A real time simulation model of glucose-insulin metabolism for type 1 diabetes patients," in *Proc. 27th IEEE Annu. Int. Conf. Eng. Med. Biol. Soc.*, 2005, pp. 298–301.

[23] D. U. Campos-Delgado, M. Hernandez-Ordonez, R. Femat, and A. Gordillo-Moscoso, "Fuzzy-based controller for glucose regulation in type-1 diabetic patients by subcutaneous route," *IEEE Trans. Biomed. Eng.*, vol. 53, no. 11, pp. 2201–2210, Nov. 2006.

[24] T. Takagi and M. Sugeno, "Derivation of fuzzy control rules from human operator's control actions," in *Proc. IFAC Symp. Fuzzy Inf. Knowl. Represent. Decision Anal.*, 1983, pp. 55–60.

[25] M. Sugeno and G. T. Kang, "Structure identification of fuzzy model," *Fuzzy Sets Syst.*, vol. 28, pp. 15–33, 1988.

[26] F. C. Erzen, G. Birol, and A. Cinar, "Glucosim: A simulator for education on the dynamics of diabetes mellitus," in *Proc. 23rd IEEE Annu. Int. Conf. Eng. Med. Biol. Soc.*, 2001, pp. 3163–3166.

[27] W. L. Tung and C. Quek, "DIC: A novel discrete incremental clustering technique for the derivation of fuzzy membership functions," presented at the 7th Pacific Rim Int. Conf. Artif. Intell., Tokyo, Japan, 2002, unpublished.

[28] C. W. Ting, "Learning convergence of TSK0-FCMAC: A novel fuzzy CMAC based on the zero-ordered TSK fuzzy inference scheme," Centre Comput. Intell., Schl. Comput. Eng., Nanyang Technol.Univ., Singapore, Tech. Rep. C2i-TR-04/003, 2004.

[29] C. W. Ting and C. Quek, "Learning convergence of TSK0-FCMAC: A localized self-organizing TSK fuzzy inference system based on CMAC structure," *Fuzzy Sets Syst.*, submitted for publication.

[30] J.-S. Ker, C.-C. Hsu, Y.-H. Kuo, and B.-D. Liu, "A fuzzy CMAC model for color reproduction," *Fuzzy Sets Syst.*, vol. 91, pp. 53–68, 1997.

[31] J. Kim and N. Kasabov, "HyFIS: Adaptive neuro-fuzzy inference systems and their application to nonlinear dynamical systems," *Neural Netw.*, vol. 12, pp. 1301–1319, 1999.

[32] J. S. R. Jang, "ANFIS: Adaptive-network-based fuzzy inference system," *IEEE Trans. Syst. Man Cybern.*, vol. 23, no. 3, pp. 665–685, May/Jun. 1993.

[33] W. L. Tung and C. Quek, "GenSoFNN: A generic self-organizing fuzzy neural network," *IEEE Trans. Neural Netw.*, vol. 13, no. 5, pp. 1075–1086, Sep. 2002.

[34] C.-J. Lin and C.-T. Lin, "An ART-based fuzzy adaptive learning control network," *IEEE Trans. Fuzzy Syst.*, vol. 5, no. 4, pp. 477–496, Nov. 1997.

[35] C. Quek and W. L. Tung, "A novel approach to the derivation of fuzzy membership functions using the Falcon-MART architecture," *Pattern Recognit. Lett.*, vol. 22, pp. 941–958, 2001.
[36] C.-T. Lin and C. S. Lee, *Neural Fuzzy Systems: A Neuro-Fuzzy Synergism on Intelligent System*. Upper Saddle River, NJ: Prentice-Hall, 1996.
[37] K. K. Ang, C. Quek, and M. Pasquier, "POPFNN-CRI(S): Pseudo outer product based fuzzy neural network using the compositional rule of inference and singleton fuzzifier," *IEEE Trans. Syst. Man Cybern. B, Cybern.*, vol. 33, no. 6, pp. 838–849, Dec. 2003.
[38] G. A. Carpenter, S. Grossberg, and D. B. Rosen, "Fuzzy ART: Fst stable learning and categorization of analog patterns by an adaptive resonance system," *Neural Netw.*, vol. 4, pp. 759–771, 1991.
[39] T. K. Kohonen, "Self-organized formation of topologically correct feature maps," *Bio. Cybern.*, vol. 43, pp. 59–69, 1982.
[40] "The effect of intensive treatment of diabetes on the development and progression of long-term complications in insulin-dependent diabetes mellitus," *New England J. Med.*, vol. 329, pp. 977–986, 1993.
[41] The National Institute of Diabetes and Digestive and Kidney Diseases (NIDDK) [Online]. Available: http://www2.niddk.nih.gov/ Accessed: Oct. 15, 2008
[42] J. A. Harris and F. G. Benedict, *A Biometric Study of Basal Metabolism in Man*. Washington, DC: Carnegie Inst. Washington, 1919.
[43] J. G. Ziegler and N. B. Nichols, "Optimum settings for automatic controllers," *Trans. ASME*, vol. 64, pp. 759–768, 1942.
[44] C. Quek and F. Yap, "Blood sampling of healthy subjects to develop and study a brain-inspired computational beta-cell," 2008, KR100011-KK Res. Grant and IDeAS/PP06-08/C2I-IDeAS Cluster Grant.

Chan Wai Ting received the B.A.Sc. degree (with honors) in computer engineering from Nanyang Technological University, Singapore, in 2001, where he is currently working towards the Ph.D. degree at the Centre of Computational Intelligence, School of Computer Engineering.

He was an Engineer with Centre of Computer Integrated Manufacturing, Sony Display Device, Singapore. His research interests include neuro-fuzzy system, associative memory, and machine learning.

Chai Quek (M'83) received the B.Sc. degree in electrical and electronics engineering and the Ph.D. degree in intelligent control from Heriot-Watt University, Edinburgh, Scotland, in 1986 and 1990, respectively.

He is an Associate Professor and a member of the Centre for Computational Intelligence, formerly the Intelligent Systems Laboratory, School of Computer Engineering, Nanyang Technological University, Singapore. His research interests include intelligent control, neuro-cognitive architectures, artificial intelligence in education, neural networks, fuzzy systems, fuzzy rule-based systems, and genetic algorithms and brain-inspired neuro-cognitive applications in computational finance and biomedical engineering.

Dr. Quek is a member of the IEEE Technical Committee on Computational Finance.